Proc. Natl. Acad. Sci. USA
Vol. 90, pp. 3192–3196, April 1993
Medical Sciences

Transgenic mouse model for neurocristopathy: Schwannomas and facial bone tumors

NIELS A. JENSEN*, MICHAEL L. RODRIGUEZ†, JUSTINE S. GARVEY*, CAROL A. MILLER†, AND LEROY HOOD*

*Division of Biology 147-45, California Institute of Technology, Pasadena, CA 91125; and †Department of Pathology, University of Southern California, Los Angeles, CA 90033

Contributed by Leroy Hood, December 31, 1992

ABSTRACT **We have characterized a strain of double transgenic mice with simian virus 40 large tumor antigen and prokaryotic *lacZ* under the control of the myelin basic protein promoter that develops spindle-cell sarcomas and osteogenic sarcomas at 5–7 months of age. Although poorly differentiated, the spindle-cell sarcomas were characterized as malignant Schwannomas based on their neural association, the presence of basal lamina, and expression of Schwann cell-specific genes. The osteogenic sarcomas were often multiple and appeared predominantly in the facial bones, less frequently in the ribs and vertebral column, and only rarely in the appendicular skeleton. Benign osteoblastic lesions were often observed adjacent to these sarcomas. Both the osteoblastic cells in the facial skeleton and Schwann cells are regarded as neural crest derivatives. The biological properties and anatomical location of these tumors suggest that they may share a common origin from the neural crest or its derivatives. R. P. Bolande [*Hum. Pathol.* (1974) 5, 409–429] introduced the term neurocristopathy as a unifying concept to describe such lesions arising from the neural crest or its derivatives. Cell lines established from both bone and Schwann cell tumors arising in these transgenic mice express simian virus 40 large tumor antigen mRNA as well as functional large tumor antigen. Such cell lines are potentially valuable in the search for markers that identify mammalian neural crest derivatives.**

Tumorigenesis is generally regarded as a multifactorial process that requires the accumulation of synergistic mutations in a number of genes involved in diverse biochemical processes such as cell division, differentiation, DNA repair, angiogenesis, and metastasis. Oncogenesis can be induced in transgenic mice harboring tumor-promoting genes, and, depending on the regulatory sequences governing transgene expression, tumors can be induced in either multiple tissues or in a single tissue (1).

In transgenic mice, the simian virus 40 (SV40) large tumor antigen (T antigen) is generally a potent carcinogen. This activity involves functional inactivation of the ubiquitously expressed tumor suppressor proteins p53 and pRb. The p53 protein, by arresting cells with damaged or mutated DNA in the G_1 phase of the cell cycle, is thought to constitute a checkpoint in DNA repair (2). In T-antigen-transformed cells, functional inactivation of p53 seems to be a major determinant of karyotype instability and an important checkpoint that must be bypassed in the clonal evolution of preneoplastic cells.

Mice harboring SV40 T antigen and prokaryotic *lacZ* under the control of the mouse myelin basic protein (MBP) promoter (MBP–SV40 T antigen and MBP–*lacZ* transgenic mice) are described elsewhere (3). The majority of these mice developed distinct hypomyelinated phenotypes. However, transgenic mice of the double transgenic strain Tn29 displayed a normal phenotype until about 5 months of age, when they present with tumors. Here we report that these tumors are malignant Schwannomas and osteogenic sarcomas (i.e., malignant mesenchymal tumors, which form bone). Interestingly, the facial bones appeared to be the most frequent site for both osteogenic sarcomas and preneoplastic osteoblastic lesions. A majority of bone-forming cells in this portion of the skeleton, like Schwann cells, are derived from the neural crest (4, 5). Thus, transgenic mice of strain Tn29 represent an interesting model for neurocristopathy—a concept introduced by Bolande (6) to describe lesions arising from alterations in migration, growth, and differentiation of cells derived from the neural crest.

MATERIALS AND METHODS

Transgenic Mice. The transgenic founder Tn29 was generated by microinjection of DNA containing purified fragments of two recombinant DNA constructs, MBP–SV40 T antigen and MBP–*lacZ*, into the pronucleus of fertilized mouse eggs (3). Tail DNA was prepared and transgenic mice were identified by blot analysis with SV40 T antigen- and *lacZ*-specific hybridization probes.

Histology and Electron Microscopy. Mice were sacrificed by an intraperitoneal overdose of tribromoethanol (Avertin) and a complete postmortem examination was performed. Fragments of tumors were processed for light and electron microscopy (see below). After the brain was removed, the facial skeleton was decalcified, sectioned in the coronal plane, and embedded *in toto*. Multiple transverse sections of the vertebral column, with the spinal cord intact, were also examined. For light microscopy, tissues were fixed in neutral phosphate-buffered 10% formalin, embedded in paraffin, and stained with hematoxylin and eosin. Sections were decalcified in RDO (American Histology Reagent, Stockton, CA). Fragments of tumor were also snap-frozen in liquid nitrogen-cooled isopentane and stored at −80°C. For electron microscopy, small fragments of fresh tumor were fixed in ice-cold Karnovsky's fixative (5% glutaraldehyde/4% paraformaldehyde), embedded in Epon, and examined with a Zeiss EM 109 electron microscope.

Cell Culture. Tumor fragments were removed aseptically and single cell suspensions were obtained by trypsin treatment for 30 min at 37°C. The tumor cells were cultured in 25-cm^2 tissue culture flasks containing Dulbecco's modified Eagle's medium (DMEM) (GIBCO) supplemented with 10% fetal bovine serum (FBS) and antibiotics in the presence or absence of dibutyryl-cAMP (DBC).

Northern Blot Analysis. Total RNA from tumor cell lines was extracted by the isothiocyanate method as described (7). For Northern blot analysis, the RNA was electrophoresed in formaldehyde/agarose gels, blotted onto nitrocellulose mem-

The publication costs of this article were defrayed in part by page charge payment. This article must therefore be hereby marked "*advertisement*" in accordance with 18 U.S.C. §1734 solely to indicate this fact.

Abbreviations: SV40, simian virus 40; T antigen, large tumor antigen; MBP, myelin basic protein; FBS, fetal bovine serum; DBC, dibutyryl-cAMP.

branes, and hybridized with ^{32}P-labeled nick-translated probes.

Immunoprecipitation of SV40 T Antigen. Semiconfluent cell cultures were incubated for 1 h in methionine-free DMEM containing 10% FBS to deplete the internal methionine pools before labeling. The cells were washed with PBS and labeled with 500 μCi of [^{35}S]methionine (1 Ci = 37 GBq) (Tran^{35}S-label; ICN) in 2 ml of methionine-free DMEM per 100-mm dish for 3–4 h with occasional rocking. At the end of the incubation, the cells were washed once with PBS at ambient temperature. The plates were drained to remove excess PBS, placed on ice, and rocked intermittently for 20–30 min with 1 ml of prechilled lysis buffer (250 mM NaCl/0.1% Nonidet P-40/50 mM Hepes, pH 7.0). The cells were scraped from the plate with a rubber policeman, transferred to a microcentrifuge tube, and centrifuged for 10 min at maximum speed at 4°C in an Eppendorf microcentrifuge. Aliquots of the supernatant (300 μl) were mixed with 500 μl of NET-N buffer (20 mM Tris·HCl, pH 8.0/100 mM NaCl/1 mM Na_2EDTA/0.1% Nonidet P-40) and 50 μl of monoclonal antibody 419 ascites fluid (gift from E. Harlow, Imperial Cancer Research Fund Laboratories, London; this antibody recognizes an N-terminal epitope of the T antigen). The mixture was incubated at 4°C for at least 1 h with rocking, after which immune complexes were precipitated with protein A-Sepharose (2 h at 4°C). The reacted protein A-Sepharose was washed five times with NET-N buffer, resuspended in 50 μl of SDS sample buffer [2% SDS/10% (vol/vol) glycerol/62 mM Tris·HCl, pH 6.8], boiled 5 min, and loaded onto SDS/10% polyacrylamide gels. The components of immunoprecipitation were resolved by electrophoresis in Tris glycine buffer together with prestained low and high molecular weight protein standards (Bio-Rad).

RESULTS

Two Tumor Phenotypes in Strain 29 Transgenic Mice. Southern blot analyses revealed that the MBP–SV40 T antigen and MBP–*lacZ* transgenes exhibited autosomal Mendelian inheritance and cosegregated in all generations of Tn29 mice. Transgenic mice of this strain appeared normal until about 5–7 months of age when tumors became apparent in various locations (Table 1). Histological examination showed these to be either poorly differentiated spindle cell sarcomas or osteogenic sarcomas (Table 1; Fig. 1).

Schwann Cell Origin of Spindle Cell Sarcomas. A total of 23 transgenic mice were examined, and 12 malignant spindle cell mesenchymal tumors (sarcomas) were present in 11 animals (Table 1). Seven of these tumors arose within nerves—2 in paravertebral spinal nerves and 5 in the trigeminal nerve (fifth cranial nerve). The tumors infiltrated peripherally within the perineurium and in several cases extended centrally to invade

Table 1. Summary of tumors and hyperplasia in strain 29 transgenic mice

Mouse	Spindle cell sarcoma	Osteogenic sarcoma	Osteoblastic hyperplasia	Chondroblastic hyperplasia
18-45	Pelvis/thigh	Rib (2)		Rib
40-1		Paranasal sinus (2)	Periodontal ligament	Periodontal ligament
41-7		Chest wall; pelvis; rib (3)		
42-11		Brain/choroid plexus; paranasal sinus (2); vertebral body (lumbar)	Paranasal sinus; periodontal ligament	
42-12		Paranasal sinus; rib	Periodontal ligament; rib	
42-14	Trigeminal nerve	Maxilla; periodontal ligament (3); rib (2)	Paranasal sinus; rib	
47-26		Paranasal sinus; periodontal ligament; rib (2)		
47-27	Axilla/shoulder			
48-21	Scapula			
56-22	Scapula	Dorsal vertebral column (cervical); paranasal sinus; rib (2)	Rib; vertebral body	
56-23		Humerus; rib	Rib	
56-24	Chest wall		Periodontal ligament; rib	Periodontal ligament
60-28		Dorsal vertebral arch (cervical)	Paranasal sinus; periodontal ligament	Periodontal ligament
60-29		Intervertebral disc (lumbar); paranasal sinus; periodontal ligament; vertebral arch (thoracic)	Periodontal ligament	Periodontal ligament
62-33			Palate; periodontal ligament	Periodontal ligament
62-35	Trigeminal nerve	Maxilla; periodontal ligament	Paranasal sinus; periodontal ligament; rib	
64-39	Trigeminal nerve	Periodontal ligament	Paranasal sinus	
65-41	Trigeminal nerve; thoracic nerve (paravertebral)			
65-42	Thoracolumbar nerve (paravertebral)			
66-43		Adjacent to trigeminal nerve; periodontal ligament	Paranasal sinus; periodontal ligament	
66-44		Paranasal sinus (2); periodontal ligament	Paranasal sinus; periodontal ligament	
67-45	Trigeminal nerve	Paranasal sinus (2); periodontal ligament (2)	Paranasal sinus; periodontal ligament	

Numbers in parentheses indicate number of individual osteosarcomas observed in a particular anatomic structure.

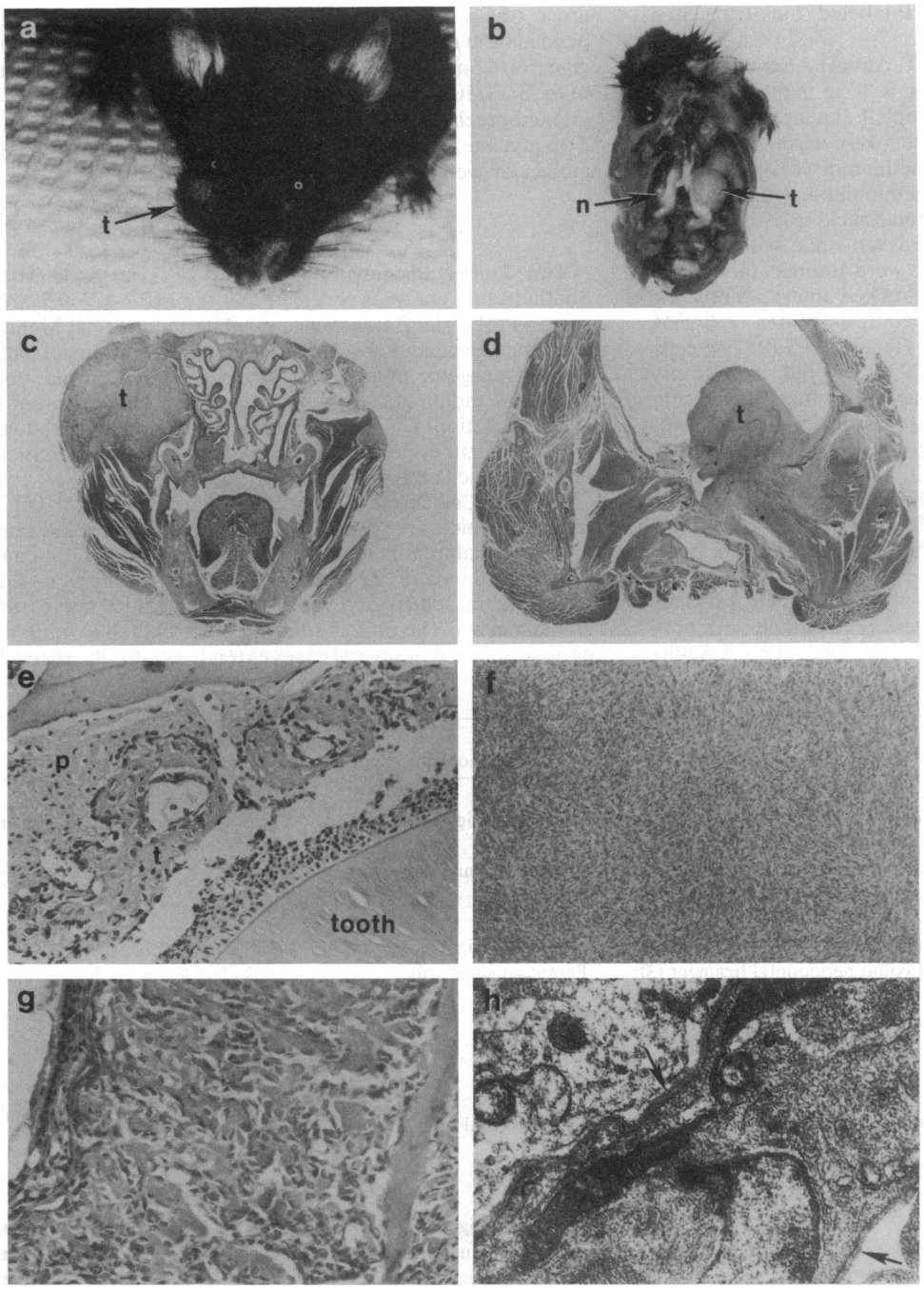

FIG. 1. Two types of tumor arise in Tn29 transgenic mice. (*a*) Mouse showing osteogenic sarcoma (t) arising from right maxilla. (*b*) Malignant Schwannoma arising in right trigeminal nerve (t). Left trigeminal nerve (n) is normal. (*c*) Coronal section through osteogenic sarcoma in *a*. Tumor (t) is well circumscribed and arises from the periosteal surface of the maxilla. (×4.25.) (*d*) Coronal section through trigeminal ganglia showing malignant Schwannoma (t) in trigeminal nerve, infiltrating the surrounding soft tissues and sphenoid bone. (×5.) (*e*) Abnormal osteoblastic proliferation in periodontal ligament. Periodontal ligament (p) is hypercellular and contains disarrayed osteoid with adjacent hyperchromatic osteoblasts (t) near the alveolar bone. Adjacent tooth is normal. (×190.) (*f*) Schwannoma showing uniform, malignant spindle cells arranged in interlacing bundles. (×20.) (*g*) Osteogenic sarcoma showing numerous disordered osteoid seams surrounded by malignant osteoblasts. (×190.) (*h*) Electron micrograph of malignant Schwannoma showing basal lamina material (arrow) and interdigitating cell processes. (×58,400.)

the subarachnoid space, and in one case the spinal cord (Fig. 1). In five cases, neural involvement could not be identified. However, all 12 spindle cell tumors appeared remarkably similar morphologically. Macroscopically, they were firm, well circumscribed, and lobulated, displaying a white to greyish cut surface. Microscopically, they were composed of hypercellular nodules of uniform spindle-shaped cells (Fig. 1*f*). There were numerous mitoses and occasional foci of necrosis. Although several tumors arose within nerves, no features were observed that suggested Schwann cell differentiation [i.e., compactly arranged spindle cells with parallel long axes—Antoni type A pattern—or loosely arranged cells widely separated by a clear matrix—Antoni type B pattern (8)]. Blood vessels were not prominent. Four of the sarcomas were examined by electron microscopy. All showed areas with elongated cells and some interdigitating processes. In addition, continuous and discontinuous basal lamina was identified in 3 of the tumors (Fig. 1*h*). These features are consistent with, but not diagnostic of, Schwann cell differentiation.

To investigate whether these tumors show Schwann cell differentiation (e.g., express Schwann cell genes) we performed Northern blot analyses on RNA extracted from tumor-derived cell lines. Cell line 56-24 was established from a spindle cell sarcoma that arose in Tn56-24 (Table 1) and showed no definite neural association. In the absence of DBC, 56-24 cells expressed moderate levels of mRNA encoding the major myelin proteins MBP and Po (Fig. 2). These genes are expressed at substantial levels in myelin-forming Schwann cells (9). A substantial downregulation of MBP and Po mRNA appeared after DBC stimulation (Fig. 2). In contrast, the Schwann cell transcription factor SCIP (10, 11) was upregulated in DBC-stimulated 56-24 cells compared to unstimulated cells (Fig. 2). MBP mRNA was also detected in another cell line, designated 64-39, established from a spindle cell sarcoma arising from the trigeminal nerve of animal

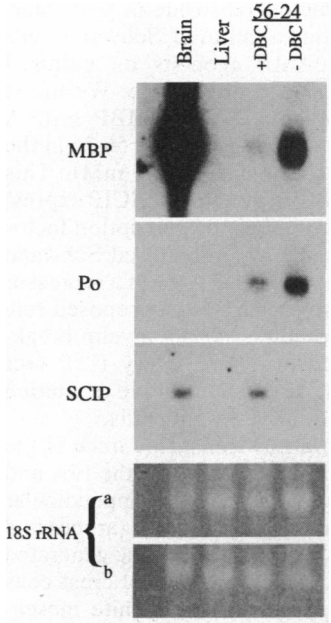

FIG. 2. Autoradiographs of Northern blot analyses of MBP, Po, and SCIP expression in uninduced and DBC-induced cells of the malignant Schwannoma cell line 56-24. Briefly, an early passage of 56-24 cells was cultured in DMEM containing 10% FBS. In the case of DBC stimulation, the cells were cultured for 3 days in the presence of 300 μM DBC before RNA purification. Control RNA from brain and liver was purified from an adult nontransgenic mouse. Ethidium bromide staining of 18S rRNA on the two blots used for hybridization indicates relative amounts of total RNA (10 μg per lane). (*a*) Filter was used in hybridization with MBP. (*b*) A second filter was used in successive hybridizations with Po and SCIP probes. All three probes were ^{32}P-labeled.

Tn64-39 (Table 1; data not shown). Thus, expression of Schwann cell-specific genes in spindle cell sarcoma-derived cell lines confirms the Schwann cell origin of these tumors.

Osteogenic Sarcomas. A total of 48 osteogenic sarcomas were found in 16 mice. Macroscopically, these tumors were hard, rounded, and gray, and they appeared to originate from the periosteal surface. In most cases, the underlying cortical bone was normal and the medullary cavity contained hematopoietic marrow. The tumors ranged from well-differentiated osteoblastic lesions with few mitoses, in which the tumor cells (osteoblasts) synthesized large amounts of mature bone (Fig. 1*g*), to poorly differentiated hypercellular lesions with sparse osteoid (uncalcified bone matrix), numerous mitotic figures, and extensive areas of necrosis. Osteoclasts (bone-resorbing cells) were demonstrated in 2 tumors.

In contrast to the malignant Schwannomas, the osteogenic sarcomas were multiple and the majority, 26, involved the facial bones including the walls of the nasal and paranasal sinuses, the mandible, and maxilla (Table 1). In the jaw, tumors arose from the alveolar bone and extended into the periodontal ligament (Fig. 1*e*). Thirteen osteogenic sarcomas arose from ribs and 5 involved the vertebral column. Only 1 tumor appeared in the appendicular skeleton (proximal humerus; Table 1). In addition, 2 osteogenic sarcomas appeared to arise within soft tissues with no obvious skeletal connection. One arose in the brain in the region of the fourth ventricle and the other was adjacent to the trigeminal ganglion (Table 1).

Frequently, the periodontal ligament adjacent to the jaw sarcomas was hypercellular, although the teeth and underlying bone appeared normal. Furthermore, a continuum from hyperplasia to overt neoplasia could be observed at this site.

The rib osteogenic sarcomas were associated with a thickened and hypercellular periosteum, which was most prominent over the anterior surfaces of the ribs. As in the facial tumors, a morphological continuum between osteoblastic hyperplasia and osteosarcoma was often apparent.

Expression of Functional T Antigen in Tumor Cells. Southern blots indicated that strain 29 mice harbor full-length copies of both injected transgenes (data not shown). Using Northern blot analyses and immunostaining, we were unable to detect T antigen and *lacZ* expression in the nervous system of these mice (data not shown). However, the frequent appearance of malignant Schwannomas suggests that the T antigen was occasionally expressed in Schwann cells.

To test whether tumor cells express T-antigen mRNA, Northern blot analyses were performed on cell lines derived from both tumor types (Fig. 3*a*). Cell lines (41-7A, 60-28, and 60-28B) were established from a pelvic osteogenic sarcoma in mouse Tn41-7 and from a similar tumor arising from the dorsal vertebral arch of mouse Tn60-28 (Table 1; Fig. 3*a*). These cell lines, as well as the two Schwannoma cell lines described above (56-24 and 64-39), were cultured in the presence or absence of DBC prior to RNA isolation and Northern blot analysis. Although the steady-state levels of T antigen mRNA varied between cell lines, this was unaffected by DBC treatment (Fig. 3*a*). Cell lines 56-24, 64-39, and 60-28B express moderate levels of T antigen mRNA, whereas cell lines 41-7 and 60-28A express high levels (Fig. 3*a*). In contrast, *lacZ* mRNA was not detected in these cell lines (data not shown).

To demonstrate the presence of functional T antigen in cell lines, coimmunoprecipitation was performed with ^{35}S-labeled cell extracts from the Schwannoma cell line 56-24 by using the monoclonal antibody mAb419 (12). This antibody coimmunoprecipitates T antigen and the tightly bound p53 protein (13). As shown in Fig. 3*b*, both the T antigen and p53 were coimmunoprecipitated, suggesting that functional T

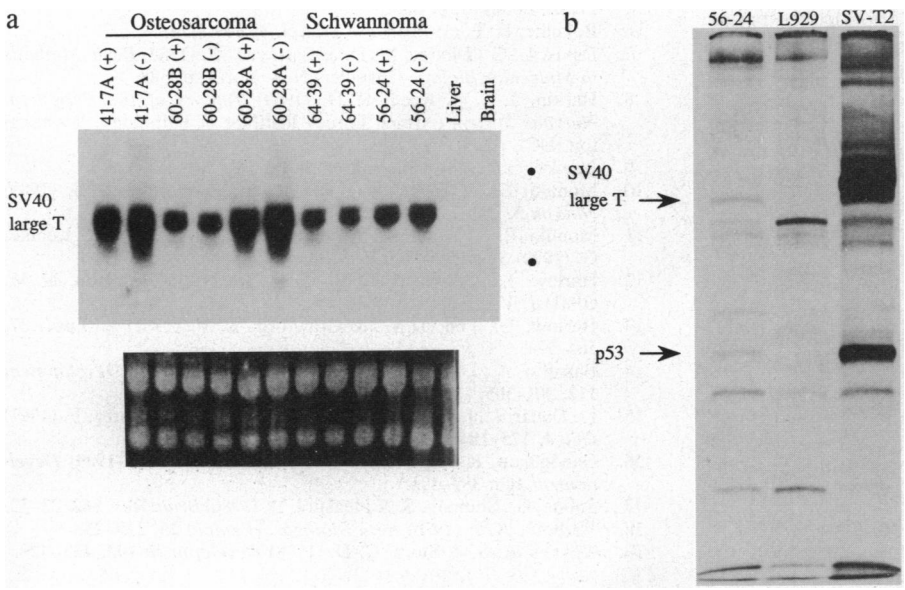

FIG. 3. (*a*) Northern blot analysis of T antigen expression in different osteosarcoma and Schwannoma cell lines derived from Tn29 mice. Early passages of the cell lines were cultured in DMEM containing 10% FBS. In the cases of DBC stimulation, the cells were cultured for 3 days in the presence of DBC (300 μM) prior to RNA purification. T-antigen-negative control RNA was purified from the brain and liver of a nontransgenic mouse. Ethidium bromide staining of 18S and 28S rRNA on the blot indicates relative amounts of total RNA (20 μg per lane). T antigen-specific hybridization probes were ^{32}P-labeled. (*b*) Coimmunoprecipitation of [^{35}S]methionine-labeled proteins of the 56-24 cell line, using an anti-T antigen monoclonal antibody. Autoradiographs are shown of immunoprecipitates from the 56-24 cell line, the L929 cell line (T antigen negative), and the SV-T2 cell line (a SV40-transformed cell line). Arrows indicate position of immunoprecipitated T antigen and coimmunoprecipitated p53 protein. Note that neither T antigen nor p53 appeared in the immunoprecipitate from the L929 cell line.

antigen is present. These findings suggest that the tumors in strain 29 mice may result from occasional expansion of a subpopulation of preneoplastic cells, which express T antigen but not the *lacZ* gene. Interestingly, although oligodendrocytes are the major site for MBP gene expression, we were unable to detect T antigen expression in the central nervous system, and, in the 23 transgenic animals examined, there was no evidence of oligodendrocyte proliferation or neoplasia (Table 1).

DISCUSSION

In this report, we characterized a strain of MBP–SV40 T antigen and MBP–*lacZ* double transgenic mice that develops an unusual tumor pattern at 5–7 months of age. Two distinct tumor types—osteogenic sarcomas and malignant Schwannomas—appeared in these mice. The facial bones and jaw were the most frequent sites for both bone tumors and preneoplastic osteo- and chondroblastic lesions. Occasionally, the preneoplastic lesions were in continuity with overt sarcomas. The malignant Schwannomas were identified on the basis of their neural location, ultrastructural features, and expression of myelin genes.

Expression of the SV40 T antigen and *lacZ* transgenes was detected in neither the central nor the peripheral nervous system of Tn29 mice. The nature of this repression is unknown. In contrast, functional T antigen was expressed at various levels in cell lines derived from both malignant Schwannomas and osteogenic sarcomas. No *lacZ* expression was detected in these cell lines. Although the selective events that led to activation of T antigen but not *lacZ* expression in tumor cells are unknown, the presence of functional T antigen in semidifferentiated Schwannoma cell lines indicates that the transgenic MBP promoter displayed some degree of tissue specificity. In contrast, although the MBP promoter was expected to be transcriptionally active in both oligodendrocytes and Schwann cells (and oligodendrocytes express high levels of MBP), oligodendrocyte tumors were not observed in strain Tn29 transgenic mice, suggesting that significant expression of the T antigen in oligodendrocytes is unlikely. Thus, differential expression of the exogenous MBP promoter in the nervous system of this transgenic model may reflect a dependence on integration site. Moreover, it is unclear why the MBP–SV40 T antigen transgene is associated with bone neoplasms. However, the majority of the bone tumors appeared in the craniofacial skeleton. Both Schwann cells and most osteo- and chrondrogenic cells in the head arise from the neural crest (4, 5). A progenitor cell giving rise to Schwann cells, satellite glial cells, and chondroblasts has been identified in primary cultures of quail cephalic neural crest cells (14, 15). The frequent appearance of craniofacial bone tumors and Schwann cell tumors in our study suggests that these two tumor types may share a common lineage, indicating that transgene expression in this model occurs in cells that are developmentally closely related. However, while these tumors represent a neurocristopathy, the lack of cell lineage markers for mammalian neural crest derivatives makes this hypothesis speculative at present. Although MBP, Po, and SCIP mRNA were present in cell lines derived from malignant Schwannomas, we were unable to detect such transcripts in bone tumor-derived cell lines (data not shown).

The Schwannoma-derived cell line 56-24 expresses moderate levels of both MBP and Po mRNA in the absence of DBC or neurons. Using a semidifferentiated Schwannoma cell line, Gandelman *et al.* (16) showed that the effects of cAMP agonists on MBP and Po mRNA are biphasic, with myelin gene expression stimulated at low doses and repressed at high doses. In contrast, cAMP agonist concentrations in the range that repress myelin gene expression are necessary for induction of galactocerebroside (a lipid characteristic of myelin) expression in cultured Schwann cells (17). Hence, the effect of cAMP agonists on cultured Schwann cells appears complex and pleiotropic. We found substantial downregulation of both Po and MBP mRNA expression in the Schwannoma-derived cell line 56-24 in the presence of a high concentration of DBC (3 mM). This downregulation correlated with upregulation of SCIP expression. SCIP is a POU domain-containing transcription factor that is upregulated by cAMP agonists in cultured Schwann cells (10). This transcription factor acts *in vitro* as a repressor of both the Po and MBP promoters and has a proposed role in downregulation of these promoters during myelin breakdown in Schwann cells following nerve injury (11). Our results are consistent with SCIP acting in negative regulation of MBP and Po gene expression in Schwann cells.

An interesting feature of strain 29 transgenic mice is the occasional appearance of osteogenic lesions in the ribs and vertebral column but their virtual absence in the appendicular skeleton. The vertebral column and its processes (arches and ribs) are generally regarded as mesodermal, being generated from somite and axial mesenchyme (18). Neural crest cells are numerous in the rostral portion of the somite mesenchyme (sclerotome) as well as in the axial mesenchyme, where they contribute neurons and Schwann cells to the developing dorsal root ganglia (19). While engulfed in a skeletogenic environment, a subset of these trunk neural crest derivatives could differentiate into bone/cartilage-forming cells and contribute to the vertebral column and processes. Experimental proof for this hypothesis awaits future investigation.

Readily established cell lines from strain 29 transgenic mice may be a valuable tool in the search for markers that identify mammalian neural crest derivatives.

We thank E. Harlow for anti-T antigen antibody and G. Lemke and C. Puckett for plasmid DNA. This work was supported by grants from National Institutes of Health (POI AG07687), National Institute of Mental Health (5-ROI-MH 39145), and National Institutes of Health (AG 05142), and by a postdoctoral fellowship (to N.A.J.) from the Alfred Benzon Foundation, Denmark.

1. Adams, M. A. & Cory, S. (1991) *Science* **254,** 1161–1167.
2. Lane, D. P. (1992) *Nature (London)* **358,** 15–16.
3. Jensen, N. A., Smith, G. M., Shine, H. D., Garvey, J. S. & Hood, L. (1993) *J. Neurosci. Res.*, 257–264.
4. Le Douarin, N. (1988) *Annu. Rev. Cell Biol.* **4,** 375–404.
5. Hall, B. K. & Hörstadius, S. (1988) *The Neural Crest* (Oxford Univ. Press, London), p. 303.
6. Bolande, R. P. (1974) *Hum. Pathol.* **5,** 409–429.
7. Davis, L. G., Dibner, M. D. & Battey, J. F. (1988) *Basic Methods in Molecular Biology* (Elsevier, New York), p. 388.
8. Harkin, J. C. & Reed, R. D. (1969) *Tumors of the Peripheral Nervous System* (Armed Forces Institute of Pathology, Washington, DC), p. 34.
9. Lemke, G. (1988) *Neuron* **1,** 535–543.
10. Monuki, E. S., Weinmaster, G., Kuhn, R. & Lemke, G. (1989) *Neuron* **3,** 783–793.
11. Monuki, E. S., Kuhn, R., Weinmaster, G., Trapp, B. D. & Lemke, G. (1990) *Science* **249,** 1300–1303.
12. Harlow, E., Crawford, L. V., Pim, D. C. & Williamson, N. M. (1981) *J. Virol.* **39,** 861–869.
13. Harlow, E., Pim, D. C. & Crawford, L. V. (1981) *J. Virol.* **37,** 564–573.
14. Baroffio, A., Dupin, E. & Le Douarin, N. M. (1991) *Development* **112,** 301–305.
15. Le Douarin, N., Dulac, C., Dupin, E. & Cameron-Curry, P. (1991) *Glia* **4,** 175–184.
16. Gandelman, K.-Y., Pfeiffer, S. E. & Carson, J. H. (1989) *Development* **106,** 389–398.
17. Sobue, G., Shuman, S. & Pleasure, D. (1986) *Brain Res.* **362,** 23–32.
18. Verbout, A. J. (1976) *Acta Biotheor. (Leiden)* **25,** 219–258.
19. Keynes, R. S. & Stern, C. D. (1988) *Development* **103,** 413–429.